ACS Catalysis

Research Article

pubs.acs.org/acscatalysis

Enhancement of Chain Growth and Chain Transfer Rates in Ethylene Polymerization by (Phosphine-sulfonate)PdMe Catalysts by Binding of $B(C_6F_5)_3$ to the Sulfonate Group

Zhengguo Cai,[†] Zhongliang Shen,[†] Xiaoyuan Zhou, and Richard F. Jordan*

Department of Chemistry, The University of Chicago, 5735 South Ellis Avenue, Chicago, Illinois 60637, United States

Supporting Information

ABSTRACT: Binding of $B(C_6F_5)_3$ to a sulfonate oxygen of (*ortho*-phosphino-arenesulfonate)PdR catalysts results in a 3−4 fold increase in the rate of chain growth and a larger increase in the rate of chain transfer. The reaction of (PO-Et)PdMe(py) (**1a**, $[PO\text{-}Et]^-$ = *ortho*-{(2-Et-Ph)$_2$P}-*para*-toluenesulfonate) with 1 equiv of $B(C_6F_5)_3$ yields the base-free dimer {(PO-Et)PdMe}$_2$ (**2a**), in which the (PO-Et)PdMe units are linked through an eight-membered $[PdSO_2]_2$ ring. The reaction of {(PO-3,5-^{t}Bu$_2$)PdMe}$_2$(TMEDA) (**4b**; $[PO\text{-}3,5\text{-}^t\text{Bu}_2]^-$ = *ortho*-{(3,5-^{t}Bu$_2$-Ph)$_2$P}-*para*-toluenesulfonate, TMEDA = *N*,*N*,*N*′,*N*′-tetramethylethylenediamine) with $BF_3{\cdot}Et_2O$ yields the soluble base-free dimer {(PO-3,5-^{t}Bu$_2$)PdMe}$_2$ (**2b**), in which the (PO-3,5-^{t}Bu$_2$)PdMe units are linked through a four-membered Pd_2O_2 ring. **2b** reacts with 2 equiv of $B(C_6F_5)_3$ to yield {[PO·B$(C_6F_5)_3$-3,5-^{t}Bu$_2$]PdMe}$_2$ (**5b**, $[PO{\cdot}B(C_6F_5)_3\text{-}3,5\text{-}^t\text{Bu}_2]^-$ = [2-{(3,5-^{t}Bu$_2$-Ph)$_2$P}-4-Me-$C_6H_3SO_2OB(C_6F_5)_3]^-$), which crystallizes from Et_2O as the monomeric complex [PO·B$(C_6F_5)_3$-3,5-^{t}Bu$_2$]PdMe(Et_2O) (**6b**). In both **5b** and **6b**, the $B(C_6F_5)_3$ binds to a sulfonate oxygen. In toluene solution at 60 °C, **2b** polymerizes ethylene (80 psi) to linear polyethylene with M_n = 3,000, while the $B(C_6F_5)_3$ adducts **5b** and **6b** yield ethylene oligomers (M_n = 160−170). **5b** and **6b** are 3−4 times more active than **2b**. Similarly, **1a** polymerizes ethylene to linear polyethylene with M_n = 29,300 (toluene, 80 °C, 435 psi), while **1a**-4 $B(C_6F_5)_3$ yields polymer with M_n = 2,520 with a 4 fold increase in activity. **2b** reacts with ethylene at 7 °C to form the ethylene adduct (PO-3,5-^{t}Bu$_2$)PdMe($CH_2{=}CH_2$) (**7b**) followed by multiple insertions to generate (PO-3,5-^{t}Bu$_2$)Pd$(CH_2CH_2)_nCH_3$ species. In contrast, **5b** reacts with ethylene to form [PO·B$(C_6F_5)_3$-3,5-^{t}Bu$_2$]PdMe($CH_2{=}CH_2$) (**8b**) followed by insertion and β-H transfer to yield propene with subsequent catalytic formation of 1-butene and higher olefins. The rate of ethylene insertion of **8b** is 3 times greater than that of **7b**, consistent with the batch polymerization results. The polymer yield and molecular weight data show that binding of $B(C_6F_5)_3$ to **2b** and **1a** increases the chain transfer rates by a factor of 80 and 42, respectively.

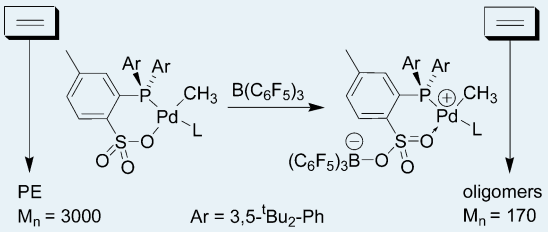

KEYWORDS: *ethylene polymerization, ethylene oligomerization, (phosphine-sulfonate)Pd catalyst, Lewis acid, remote binding*

INTRODUCTION

Palladium(II) alkyl complexes that contain *ortho*-phosphino-arenesulfonate ligands ($[PO]^-$, **A**, Chart 1) have attracted significant attention because of their unique characteristics as olefin polymerization catalysts.[1,2] (PO)PdR(L) species (L = labile ligand) polymerize ethylene to linear polyethylene and copolymerize ethylene with a wide variety of polar vinyl monomers to functionalized linear polymers.[3−18] However, (PO)PdR(L) catalysts generally display mediocre performance in ethylene homopolymerization, and, while polar monomers are incorporated, they normally exert a deleterious effect on polymerization activity and molecular weight. Therefore, it is important to investigate strategies for enhancing the performance of (PO)PdR(L) catalysts.[19−21]

Chart 1

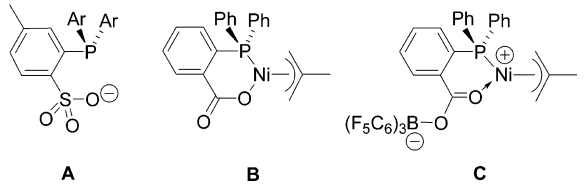

Bazan showed that binding of $B(C_6F_5)_3$ to the carbonyl oxygen of the SHOP-type ethylene oligomerization catalyst [κ^2-*P*,*O*-$Ph_2PC_6H_4CO_2$]Ni(η^3-CH_2CMeCH_2) (**B**, Chart 1) generates the zwitterionic species [κ^2-*P*,*O*-$Ph_2PC_6H_4C$(OB$(C_6F_5)_3$)O]Ni(η^3-CH_2CMeCH_2) (**C**, Chart 1), which is substantially more reactive in ethylene oligomerization than **B**. The improved activity was attributed to the removal of electron density from the Ni center by the remotely bound Lewis acid.[22−24] This approach has been used to modulate the activity and selectivity of Ni catalysts that contain carboxamidate,[25−27] enamide, and other ligands that contain sites for remote Lewis acid binding.[28−32] Here we report that binding of

Received: March 2, 2012
Revised: March 31, 2012
Published: April 18, 2012

$B(C_6F_5)_3$ to a sulfonate oxygen of (PO)PdR(L) catalysts increases both the chain growth rate and the chain transfer rate in ethylene polymerization by these systems.

RESULTS AND DISCUSSION

Abstraction of Pyridine from (PO)PdMe(py) Species by $B(C_6F_5)_3$. In previous work we showed that (PO)PdR(py) complexes react with 1 equiv of $B(C_6F_5)_3$ to generate $B(C_6F_5)_3$(py) and dimeric base-free $\{(PO)PdMe\}_2$ species.[6] However, the isolated base-free dimers usually exhibit poor solubility, which complicates studies of their reactivity. For example, abstraction of pyridine from (PO-Et)PdMe(py) (**1a**, $[PO\text{-}Et]^-$ = *o*-{(2-Et-Ph)$_2$P}-*p*-toluenesulfonate) with 1 equiv of $B(C_6F_5)_3$ in CH_2Cl_2 generates $B(C_6F_5)_3$(py) and the base-free species (PO-Et)PdMe, which slowly crystallizes as the dimer $\{(PO\text{-}Et)PdMe\}_2$ (**2a**, eq 1). The isolated dimer is insoluble in CH_2Cl_2.

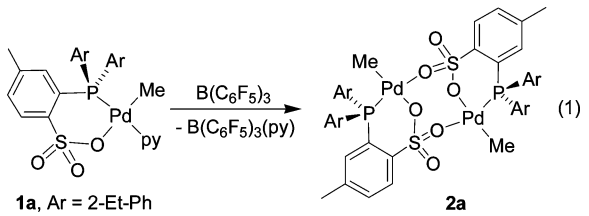

X-ray crystallographic analysis shows that **2a** exists as a sulfonate-bridged dimer in the solid-state (Figure 1). One

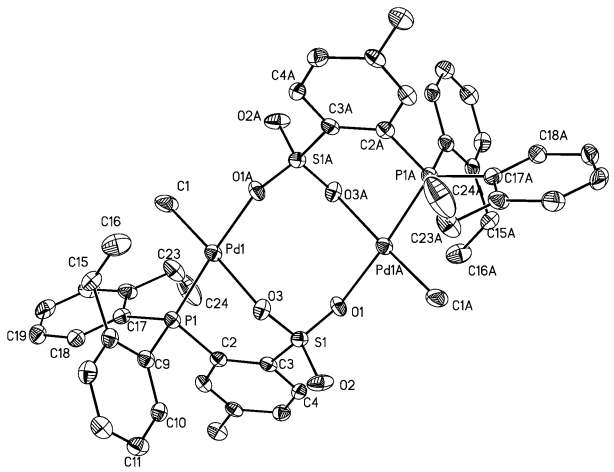

Figure 1. Molecular structure of $\{(PO\text{-}Et)PdMe\}_2$ (**2a**). Hydrogen and solvent atoms are omitted. Selected bond lengths (Å) and angles (deg): Pd(1)−O(1A) 2.155(3), Pd(1)−O(3) 2.170(2), Pd(1)−C(1) 2.005(4), Pd(1)−P(1) 2.2007(16), S(1)−O(1) 1.469(2), S(1)−O(2), 1.426(2), S(1)−O(3) 1.462(3), O(1A)−Pd(1)−O(3) 89.59(10), O(1A)−Pd(1)−C(1) 90.82(13), C(1)−Pd(1)−P(1) 95.50(12), O(3)−Pd(1)−P(1) 83.77(8), Pd(1)−O(3)−S(1) 121.93(13), Pd(1)−O(1A)−S(1A) 128.84(14).

oxygen of a given (PO-Et)PdMe unit participates in the (PO)Pd chelate and a different oxygen coordinates to the Pd in the other (PO-Et)PdMe unit. The resulting central eight-membered ring adopts a chair conformation, with O(1), S(1), O(3), O(1A), S(1A), and O(3A) forming a plane and Pd(1) and Pd(1A) lying on opposite sides this plane. The geometry at palladium is square planar, and the (PO)Pd chelate ring is puckered, with one P-*(2-Et-Ph)* group occupying a pseudo-axial position and the other a pseudo-equatorial position. An analogous structure was observed for {[*o*-{(2-OMe-Ph)$_2$P}-*p*-toluenesulfonate]Pd(CH_2SiMe_3)}$_2$.[6]

{(PO-3,5-^{t}Bu$_2$)PdMe}$_2$. A more soluble $\{(PO)PdMe\}_2$ system was developed based on the *o*-{(3,5-^{t}Bu$_2$-Ph)$_2$P}-*p*-toluenesulfonate ligand ($[PO\text{-}3,5\text{-}^t\text{Bu}_2]^-$). The neutral compound [PO-3,5-^{t}Bu$_2$]H (**3b**) was prepared by sequential addition of 1 equiv of dilithiated *p*-toluenesulfonic acid and 2 equiv of Li[3,5-^{t}Bu$_2$-Ph] to PCl_3 followed by protonation with HCl. **3b** exists as a zwitterion in CD_2Cl_2 based on the large P−H NMR coupling constant ($^1J_{PH}$ = 570 Hz). The reaction of **3b** with (TMEDA)$PdMe_2$ (TMEDA = *N,N,N′,N′*-tetramethylethylenediamine) generates $\{(PO\text{-}3,5\text{-}^t\text{Bu}_2)PdMe\}_2$(TMEDA) (**4b**), in which the two (PO-3,5-^{t}Bu$_2$)PdMe units are bridged by the TMEDA ligand (Scheme 1).[7] **4b** reacts with pyridine to form the monomeric complex (PO-3,5-^{t}Bu$_2$)PdMe(py) (**1b**).

Scheme 1

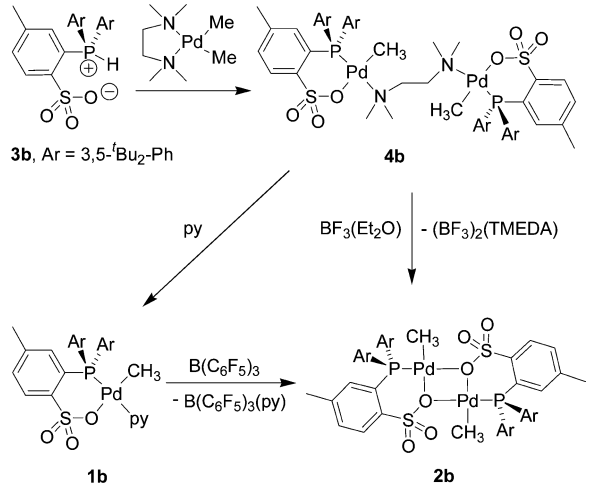

The conventional method of using $B(C_6F_5)_3$ to abstract the pyridine ligand from **1b** cleanly generates the base-free dimer $\{(PO\text{-}3,5\text{-}^t\text{Bu}_2)PdMe\}_2$ (**2b**), along with $B(C_6F_5)_3$(py). These species could not be separated because of their similar solubilities. However, **4b** reacts cleanly with $BF_3{\cdot}Et_2O$ to form **2b** and the insoluble adduct $(BF_3)_2$(TMEDA), which can be removed by simple filtration.[33−35] This method provides access to **2b** in large quantities and high purity (Scheme 1).

The solid state structure of **2b** is shown in Figure 2. The two (PO-3,5-^{t}Bu$_2$)PdMe units are linked through a four-membered Pd−O−Pd-O ring. The same oxygen that participates in a given (PO)Pd chelate ring to form a (PO-3,5-^{t}Bu$_2$)PdMe unit (O(1)) also binds to the Pd in the other (PO-3,5-^{t}Bu$_2$)PdMe unit to form the central Pd−O−Pd−O core. The O−Pd−O angle within the central ring is 77.86(9)°, resulting a slightly distorted square planar geometry at Pd. The six-membered (PO)Pd chelate ring adopts a puckered conformation. The difference between the structures of **2b** and **2a** can be rationalized based on steric effects. Dimerization of the (PO-3,5-^{t}Bu$_2$)PdMe units in **2b** occurs through the Pd-bound oxygen to form the 4-membered ring structure because this oxygen carries a higher negative charge than the other oxygens. In contrast, for **2a**, the *ortho*-Et substituents prevent close approach of the (PO-Et)PdMe units and dimerization occurs through the non-Pd-bound oxygens, resulting in the 8-membered ring structure.

Several lines of evidence establish that **2b** exists as a dimer in CD_2Cl_2 solution. First, the ^{1}H and ^{31}P{^{1}H} NMR spectra of **2b**

dx.doi.org/10.1021/cs300147c | ACS Catal. 2012, 2, 1187−1195

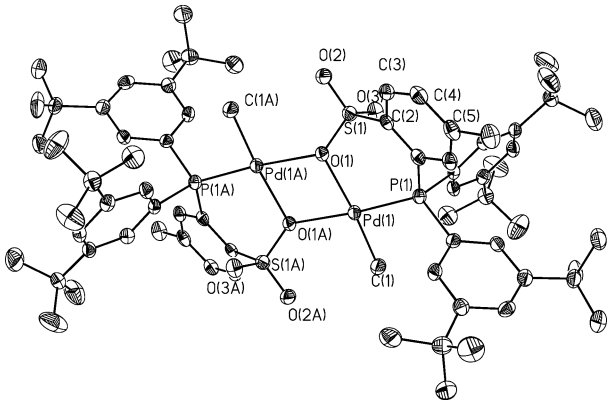

Figure 2. Molecular structure of $\{(PO\text{-}3,5\text{-}^tBu_2)PdMe\}_2$ (**2b**). Hydrogen atoms are omitted. Selected bond distances (Å) and angles (deg): Pd(1)−O(1) 2.204(2), Pd(1)−O(1A) 2.181(2), Pd(1)−C(1) 2.006(3), Pd(1)−P(1) 2.1811(10), S(1)−O(1) 1.511(2), S(1)−O(2), 1.429(2), S(1)−O(3) 1.436(2), O(1A)−Pd(1)−O(1) 77.86(9), O(1A)−Pd(1)−C(1) 97.25(12), C(1)−Pd(1)−P(1) 87.77(11), O(1)−Pd(1)−P(1) 97.12(6), Pd(1)−O(1)−Pd(1A) 102.14(9).

in CD_2Cl_2 at different concentrations are identical. This result argues against the possibility of **2b** being in rapid equilibrium with a monomeric $(PO\text{-}3,5\text{-}^tBu_2)PdMe(CD_2Cl_2)$ solvent adduct, since the fraction of the latter species is expected to increase with decreasing total Pd concentration, resulting in a change in the observed NMR spectra. Second, APCI-MS spectra of **2b** in CH_2Cl_2 show predominant peaks due to the dimer. Finally, the hydrodynamic volume of **2b** in CD_2Cl_2 solution at 23 °C determined by Pulsed Gradient Spin Echo (PGSE) NMR (3.32 nm^3), is similar to that of the dinuclear species **4b** (3.12 nm^3), and about twice as large as that of **1b** (1.65 nm^3).[20]

The ambient temperature ^1H NMR spectra of **1b**, **2b**, and **4b** each contain one set of 3,5-^{t}Bu$_2$-Ph resonances, consistent with rapid inversion of the $(PO\text{-}3,5\text{-}^tBu_2)Pd$ chelate rings.[5,6]

Binding of $B(C_6F_5)_3$ to $(PO\text{-}3,5\text{-}^tBu_2)PdMe$ Species. The reaction of the base-free dimer **2b** with 2 equiv of $B(C_6F_5)_3$ (i.e., one equiv per Pd) in CH_2Cl_2 at room temperature affords the adduct $\{[PO{\cdot}B(C_6F_5)_3\text{-}3,5\text{-}^tBu_2]PdMe\}_2$ ($[PO{\cdot}B(C_6F_5)_3\text{-}3,5\text{-}^tBu_2]^-$ = $[2\text{-}\{(3,5\text{-}^tBu_2\text{-}Ph)_2P\}\text{-}4\text{-}Me\text{-}C_6H_3SO_2OB(C_6F_5)_3]^-$, **5b**, Scheme 2). Crystallization of **5b** from Et_2O yields the monomeric complex $[PO{\cdot}B(C_6F_5)_3\text{-}3,5\text{-}^tBu_2]PdMe(Et_2O)$ (**6b**).

X-ray crystallographic analysis of **6b** establishes that the $B(C_6F_5)_3$ unit is bound to a sulfonate oxygen (Figure 3). Comparison of the S−OPd distance (S(1)−O(2) = 1.455(13) Å) and the S−OB distance (S(1)−O(4) = 1.5101(13) Å) to values for typical S=O double bonds (1.42 Å) and S−O single bonds (1.56 Å),[36] implies that **6b** is best represented by the zwitterionic resonance structure in Scheme 2. The B−OS distance (B(1)−O(4) = 1.561(2) Å) is intermediate between that of a B−O single bond (e.g., $[Cp_2Ta(OH)Me][HOB(C_6F_5)_3]$, 1.490(10) Å)[37] and a B−O dative bond (e.g., $PhC(OEt)O{\rightarrow}B(C_6F_5)_3$, 1.594(5) Å),[38] and similar to the B−OC distance in **C** (1.541(5) Å).[22]

Solution Structures and Dynamics of $[PO{\cdot}B(C_6F_5)_3\text{-}3,5\text{-}^tBu_2]PdMe$ Species. The ^{19}F and ^{11}B NMR resonances of **6b** are strongly shifted from those of free $B(C_6F_5)_3$ and appear at similar chemical shifts as those for other adducts of $B(C_6F_5)_3$ and oxygen-based ligands, for example, $(C_6F_5)_3B(O{=}CR_2)$[38] and $(C_6F_5)_3B(O{=}C\{O(CH_2)_4\text{-}\})$.[39] These results indicate that

Scheme 2

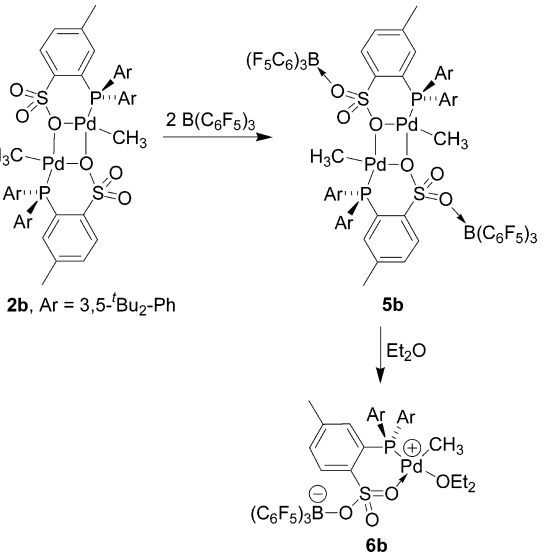

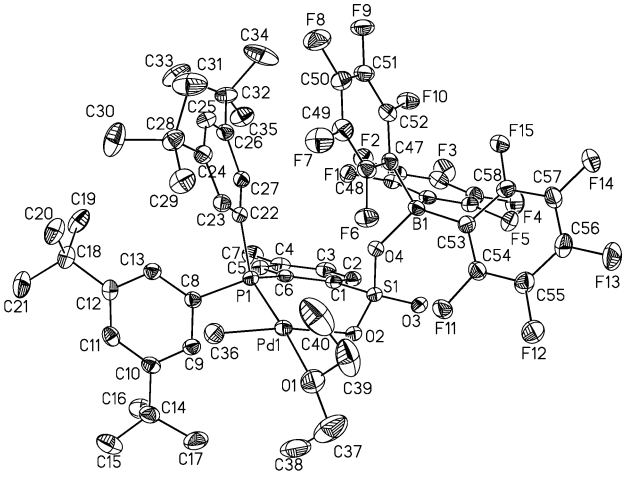

Figure 3. Molecular structure of **6b**. Hydrogen atoms are omitted. Selected bond distances (Å) and angles (deg): Pd(1)−C(36) 2.0104(19), Pd(1)−P(1) 2.1827(6), Pd(1)−O(1) 2.1689(15), Pd(1)−O(2) 2.1780(13), S(1)−O(2) 1.455(13), S(1)−O(3) 1.4274(13), S(1)−O(4) 1.5101(13), B(1)−O(4) 1.561(2), O(2)−Pd(1)−P(1) 94.79(4), C(36)−Pd(1)−O(1) 86.61(7), C(36)−Pd(1)−P(1) 88.89(6), O(1)−Pd(1)−O(O2) 89.75(5), C(47)−B(1)−C(53) 106.98(15), C(47)−B(1)−C(41) 114.70(15), C(53)−B(1)−C(41) 113.97(16), O(4)−B(1)−C(47) 102.26(14), O(4)−B(1)−C(53) 111.12(15), O(4)−B(1)−C(41) 107.22(15).

the $B(C_6F_5)_3$-sulfonate binding is retained in solution. The ^{19}F and ^{11}B NMR data for **5b** are very similar to those of **6b**, consistent with binding of the $B(C_6F_5)_3$ to the sulfonate group.

The ^1H NMR spectra of **5b** and **6b** each contain one set of 3,5-^{t}Bu$_2$-Ph resonances at −60 °C. In contrast to the situation for **1b**, **2b**, and **4b**, this result cannot be realized by simple inversion of the $[PO{\cdot}B(C_6F_5)_3\text{-}3,5\text{-}^tBu_2]Pd$ chelate ring since, because of the presence of the O-bound $B(C_6F_5)_3$ unit, the 3,5-^{t}Bu$_2$-Ph rings remain diastereotopic even in the presence of rapid chelate ring inversion. Therefore, some dynamic process that inverts the configuration at S must occur. Two likely exchange pathways are shown in Scheme 3. Pathway 1 involves intermolecular exchange of $B(C_6F_5)_3$ via B−O cleavage, and pathway 2 involves intramolecular exchange of Pd between

dx.doi.org/10.1021/cs300147c | ACS Catal. 2012, 2, 1187−1195

Scheme 3

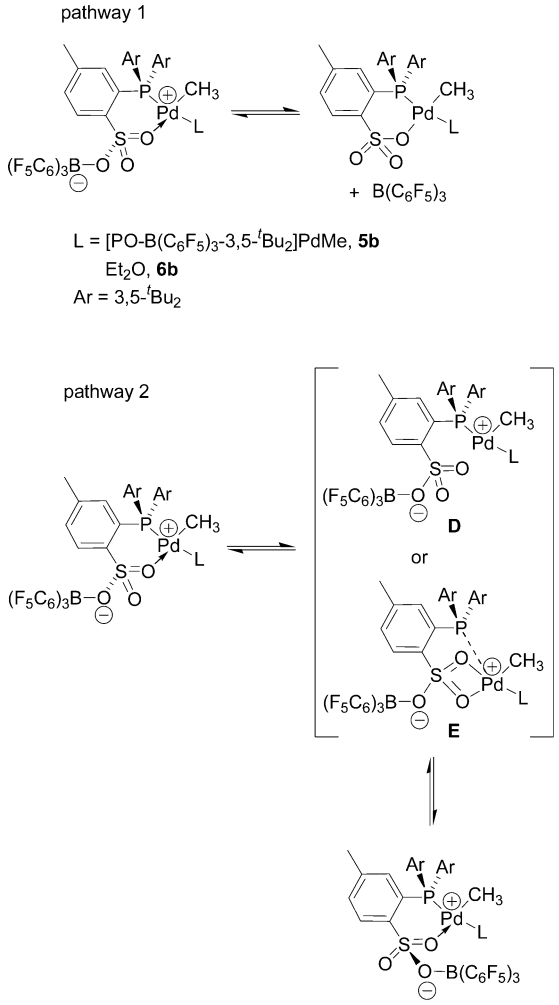

sulfonate oxygens, for example, by a dissociative (via **D**) or nondissociative (via **E**) mechanism. The ^{19}F NMR spectrum of **5b** in the presence of excess $B(C_6F_5)_3$ at −40 °C contains separate sharp resonances for free and coordinated $B(C_6F_5)_3$, indicating that intermolecular $B(C_6F_5)_3$ exchange is slow on the NMR time scale. However, under these conditions, the ^{1}H spectrum contains one set of 3,5-^{t}Bu$_2$-Ph resonances. These results provide strong evidence for the operation of pathway 2.

It is difficult to distinguish the dissociative and nondissociative mechanisms in pathway 2. On the basis of DFT calculations, Nozaki and Morokuma proposed that cis/trans isomerization of (PO)PdMe(L) species proceeds via intermediates that are similar to **E** in pathway 2.[12] The addition of excess $B(C_6F_5)_3$ to **6b** in CD_2Cl_2 solvent yields $B(C_6F_5)_3(Et_2O)$ and **5b**.

Ethylene Polymerization and Oligomerization. Ethylene polymerization results are summarized in Table 1. At 60 °C, base-free dimer **2b** yields low molecular-weight polyethylene (PE, M_n = 3000) with an activity of 110 kg PE/mol·h (entry 1). In contrast, the $B(C_6F_5)_3$-coordinated complex **5b** generates primarily ethylene oligomers (M_n = 170, determined by ^{1}H NMR) along with a small amount of PE (entry 2). The activity of **5b** is about three times higher than that of **2b**. The production of a mixture of oligomers and polymer suggests that under these polymerization conditions, **5b** and/or the [PO·B-$(C_6F_5)_3$-3,5-^{t}Bu$_2$]PdR(C_2H_4) active species derived from **5b** undergo partial dissociation of $B(C_6F_5)_3$ to generate the same (PO-3,5-^{t}Bu$_2$)PdR(C_2H_4) active species that is formed from **2b**, which produces the polymer. Consistent with this explanation, the catalyst generated from **5b** with 3 equiv of $B(C_6F_5)_3$ added to suppress the $B(C_6F_5)_3$ dissociation produces only ethylene oligomers with a higher activity than **5b** alone (entry 3). Similar results are obtained with diethyl ether adduct **6b** and pyridine adduct **1b** (entries 4−6). For example, the base-free (PO-3,5-^{t}Bu$_2$)PdR catalyst produced by the in situ reaction of **1b** and 1 equiv of $B(C_6F_5)_3$ produces PE with M_n = 2700 (entry 5), while addition of 3 more equiv of $B(C_6F_5)_3$ generates a catalyst that produces only ethylene oligomers with a 3−4 fold increase in activity (entry 6). These results show that remote binding of $B(C_6F_5)_3$ to a sulfonate oxygen of (PO-3,5-^{t}Bu$_2$)PdR species increases the yield and strongly decreases the molecular weight of polyethylene produced by these catalysts.

The oligomers produced by [PO·$B(C_6F_5)_3$-3,5-^{t}Bu$_2$]PdR catalysts display a Schulz−Flory distribution (Figure 4), consistent with single site catalysis.[40−42] The **5b**-3 $B(C_6F_5)_3$ (entry 3) and **6b**-3 $B(C_6F_5)_3$ (entry 4) catalysts exhibit similar Schulz−Flory α and β values. The α and β values for **1b**-4 $B(C_6F_5)_3$ (entry 6) are slightly different, possibly because of the presence of $B(C_6F_5)_3$(py), which is formed in situ. The oligomers are mostly 1-alkenes (81%), with 11% internal olefins and 8% 1,1-disubstituted olefins.

To explore if the effects of $B(C_6F_5)_3$ on ethylene polymerization by (PO)PdR catalysts are general, we studied the (PO-Et)PdMe system. Ethylene polymerization results for catalysts

Table 1. Ethylene Polymerization with (PO)PdMe(L) and [PO·$B(C_6F_5)_3$]PdMe(L) Catalysts

entry	catalyst	$B(C_6F_5)_3$ (equiv vs Pd)	yield of oligomer (g)[b]	yield of polymer (g)[c]	activity (kg/mol·h)	M_n	M_w/M_n	α[d]	β[d]
1[a]	**2b**	0	trace	0.57	110	3000[c]	2.0		
2[a]	**5b**	0	1.70	0.08	360	170[b]			
3[a]	**5b**	3	2.34	0.00	470	160[b]		0.76	0.32
4[a]	**6b**	3	2.51	0.00	500	170[b]		0.79	0.27
5[a]	**1b**	1	trace	0.61	120	2700[c]	2.0		
6[a]	**1b**	4	2.22	0.00	440	130[b]		0.65	0.54
7[e]	**1a**	1	0	1.57	1570	29,300[c]	2.2		
8[e]	**1a**	2	0	3.87	3870	19,600[c]	1.9		
9[e]	**1a**	4	trace	5.65	5650	2,520[c]	2.5		

[a]Polymerization conditions: toluene = 50 mL, Pd = 10 μmol, ethylene = 80 psi, temperature = 60 °C, time = 30 min. [b]Yield of product that is soluble in toluene at room temperature; yield and molecular weight determined by ^{1}H NMR of reaction mixture. [c]Yield of product that is insoluble in toluene at room temperature; molecular weight determined by GPC using universal calibration. [d]α = rate of propagation/(rate of propagation + rate of chain transfer); β = rate of chain transfer/rate of propagation. [e]Polymerization conditions: toluene = 50 mL, Pd = 1.0 μmol, ethylene = 435 psi, temperature = 80 °C, time = 1 h.

dx.doi.org/10.1021/cs300147c | ACS Catal. 2012, 2, 1187−1195

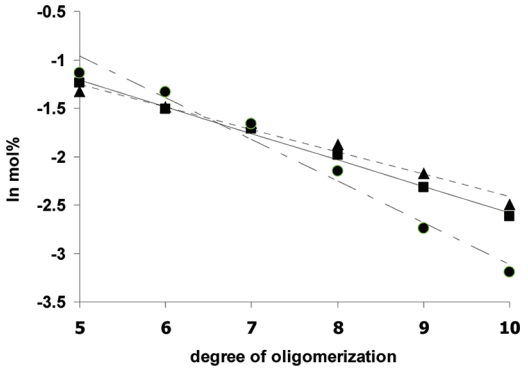

Figure 4. Schulz–Flory plots for the oligomers produced by **5b**-3 $B(C_6F_5)_3$ (■, Table 1, entry 3), **6b**-3 $B(C_6F_5)_3$ (▲, entry 4), and **1b**-4 $B(C_6F_5)_3$ (●, entry 6).

generated by in situ addition of varying amounts of $B(C_6F_5)_3$ to **1a** at 80 °C are summarized in entries 7–9 of Table 1. Addition of 1 equiv of $B(C_6F_5)_3$ to **1a** generates base-free (PO-Et)PdMe, which displays an activity of 1570 kg PE/mol·h and yields PE with M_n = 29,300 (entry 7). Addition of more $B(C_6F_5)_3$ results in a progressive increase in activity and decrease in polymer molecular weight (entries 8, 9). Interestingly, the polydispersity of the PE product remains close to 2 as the level of $B(C_6F_5)_3$ is increased. This result suggests that under these polymerization conditions (80 °C), active (PO-Et)PdR and (PO·$B(C_6F_5)_3$-Et)PdR species are in fast equilibrium on the time scale of the lifetime of a growing chain, so that the system behaves like a single site catalyst.

Ethylene Insertion and *β*-H Transfer Rates. The most likely cause of the increase in the yield of polymer/oligomer that results from binding of $B(C_6F_5)_3$ to the (PO)PdR catalysts is an increase in the chain growth rate. To address this issue, ethylene insertion reactions were investigated by NMR. The reaction of base free dimer **2b** with ethylene at low temperature (below 0 °C) results in partial reversible formation of the ethylene complex (PO-3,5-^{t}Bu$_2$)PdMe(C_2H_4) (**7b**, Scheme 4). The ^{31}P NMR chemical shift of **7b** (δ 16.0), which contains a soft ethylene ligand trans to the phosphine, is significantly different from those of **1b** (δ 30.5), **2b** (δ 33.0), and **6b** (δ 34.5), which contain hard nitrogen or oxygen ligands in this position. Even at −90 °C, exchange of free and coordinated ethylene is fast on the NMR time scale, so that only one

Scheme 4

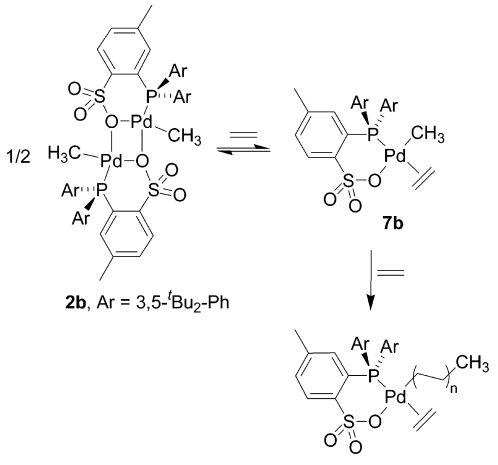

averaged ethylene signal is observed in the ^{1}H and ^{13}C NMR spectra of **7b**. However, exchange of **2b** and **7b** is slow on the NMR time scale at −50 °C.

2b is completely converted to **7b** in the presence of a large excess of ethylene (86 equiv vs Pd) at 7 °C. At this temperature, **7b** undergoes multiple ethylene insertions to generate a mixture of (PO-3,5-^{t}Bu$_2$)Pd{(−CH_2CH_2−)$_n$Me} species. The ^{1}H NMR spectrum of the mixture contains a new set of resonances for the [PO-3,5-^{t}Bu$_2$]$^-$ ligand that differ from those of **7b**, and broad resonances in the δ 1.3–0.6 region because of the alkyl chains. The alkyl resonances are very similar to those observed for [*o*-{(2-OMe-Ph)$_2$P}-benzenesulfonate]Pd({CH_2CH_2R})(2,6-lutidine) species with long alkyl chains.[12] The first-order rate constant for the consumption of **7b** measured by the disappearance of the Pd*Me* resonance is $k_{insert,\ 7b}$ = 1.1 × 10^{-4} s^{-1} at 7 °C. After 47 min, a white solid formed, which is a mixture of (PO-3,5-^{t}Bu$_2$)Pd(R)-(C_2H_4) species with long alkyl chains. At this stage, 23 mol % of **7b** was consumed and about 3 equiv of ethylene was consumed. These results indicate that the ethylene insertion of the higher alkyl (PO-3,5-^{t}Bu$_2$)Pd((−CH_2CH_2−)$_n$Me)(C_2H_4) species is faster than that of **7b**.

In contrast, ^{1}H NMR monitoring of the reaction of $B(C_6F_5)_3$ adduct **5b** with excess ethylene at 7 °C reveals the initial formation of ethylene adduct **8b**, followed by the disappearance of this species and the formation of Pd–Pr and Pd–Et species, with concomitant formation of propene and catalytic formation of 1-butene and higher *α*-olefins (Scheme 5). The first-order

Scheme 5

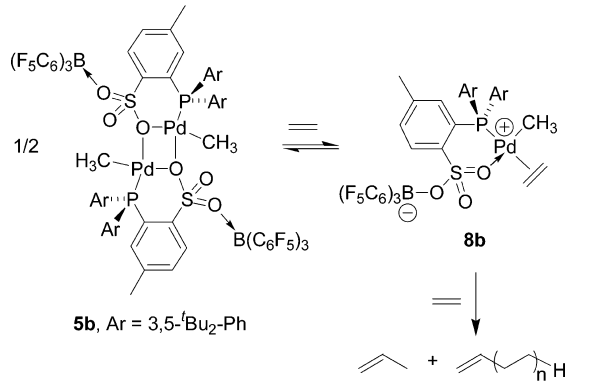

rate constant for the consumption of **8b** determined from the disappearance of the Pd-*Me* resonance is $k_{insert,\ 8b}$ = 3.0 × 10^{-4} s^{-1} at 7 °C, about three times larger than the value measured for **7b**. After 20 min, 26 mol % of **8b** was consumed and over 6 equiv of ethylene was consumed, producing 0.19 equiv of propene, 2.3 equiv of 1-butene, 0.25 equiv of 2-butenes (from isomerization of 1-butene), and 0.80 equiv of higher *α*-olefins. These results are consistent with insertion of **8b** to generate a [PO·$B(C_6F_5)_3$-3,5-^{t}Bu$_2$]PdPr species, followed by rapid *β*-H transfer to release propene and subsequent oligomerization of ethylene by an insertion/*β*-H transfer process. These results also confirm that binding of $B(C_6F_5)_3$ to the sulfonate oxygen of (PO)PdR catalysts increases both the ethylene insertion rate and the *β*-H transfer rate.

The increase in the chain transfer rate that results from binding of $B(C_6F_5)_3$ can be estimated from eq 2, in which X_n, R_g and R_t are the number average degree of polymerization, growth rate, and chain transfer rate for the (PO)PdR catalyst,

dx.doi.org/10.1021/cs300147c | *ACS Catal.* 2012, 2, 1187–1195

and $X_{n,B}$, $R_{g,B}$ and $R_{t,B}$ are the corresponding values for the $B(C_6F_5)_3$ adduct. Assuming that the growth rates are proportional to the polymer/oligomer yields, the data in Table 1 show that binding of $B(C_6F_5)_3$ to **2b** and **1a** increases the chain transfer rates by a factor of 80 (entry 3 vs 1) and 42 (entry 9 vs 7) respectively.

$$R_{t,B}/R_t = X_n R_{g,B}/X_{n,B} R_g \quad (2)$$

Comparison with Other Systems. The binding of $B(C_6F_5)_3$ to a sulfonate oxygen of a (PO)PdRL species weakens the Pd−O bond and increases the electrophilic character of the Pd center. Indeed, X-ray structural data show that $[PO{\cdot}B(C_6F_5)_3\text{-}3,5\text{-}{}^tBu_2]PdMe(Et_2O)$ (**6b**) is best described as a zwitterion with a positive charge at Pd, and $[PO{\cdot}B(C_6F_5)_3]PdR(ethylene)$ species should have similar charge distributions. These effects result in a 3 to 4-fold increase in chain growth rates and a 40 to 80-fold increase in chain transfer rates in ethylene polymerization/oligomerization by $[PO{\cdot}B(C_6F_5)_3]PdR$ catalysts. The dramatic increase in chain transfer rates is in accordance with earlier observations that related cationic Pd catalysts such as $\{{}^tBu_2PCH_2C(=O)Ph\}$-$PdRL^+$, $\{Ar_2PCH_2C(=O)Ar\}PdRL^+$ and $(PR_3)Pd(allyl)$-$(L)^+$,[43−45] as well as zwitterionic $\{o\text{-}Ph_2P{-}C_6H_4BF_3\}PdMe(L)$ species,[46,47] exhibit fast chain transfer rates and function as ethylene oligomerization catalysts.

EXPERIMENTAL SECTION

General Procedures. All experiments were performed using drybox or Schlenk techniques under a nitrogen atmosphere. Nitrogen was purified by passage through activated molecular sieves and Q-5 oxygen scavenger. CD_2Cl_2 was distilled from P_2O_5. Other deuterated solvents were purchased from Cambridge Isotope Laboratories and used as received. Hexanes, diethyl ether, toluene, and methylene chloride were purified by passage through activated alumina and BASF R3−11 oxygen scavenger. Ethylene (polymer grade) was purchased from Matheson Trigas and used as received. Complex **1a** and $(TMEDA)PdMe_2$ were synthesized by literature procedures.[6]

NMR spectra of organometallic complexes were recorded on Bruker DMX-500 or DRX-400 spectrometers in Teflon-valved tubes at ambient temperature unless otherwise indicated. ^1H and ^{13}C chemical shifts are reported relative to $SiMe_4$ and were determined by reference to the residual ^1H and ^{13}C solvent resonances. ^{31}P NMR spectra were referenced externally to H_3PO_4/D_2O (δ 0). ^{19}F spectra were referenced externally to $CFCl_3$ (δ 0). Coupling constants are given in hertz (Hz). The numbering scheme for NMR assignments is given in Figure 5.

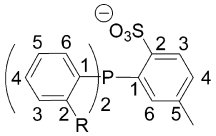

Figure 5. Numbering scheme used for NMR assignments.

Electrospray mass spectra (ESI-MS) and atmospheric pressure chemical ionization mass (APCI-MS) were recorded on freshly prepared samples (ca. 1 mg/mL in CH_2Cl_2) using an Agilent 1100 LC-MSD spectrometer. Typical instrumental parameters were as follows: drying gas temperature 350 °C, nebulizer pressure 35 psi, drying gas flow 12.0 L/min, and fragmentor voltage 0, 70, or 100 V. The observed isotope patterns closely matched calculated isotope patterns. The listed m/z value corresponds to the most intense peak in the isotope pattern.

$\{$(PO-Et)PdMe$\}_2$ (2a). A flask was charged with (PO-Et)PdMe(py) (1.32 g, 2.16 mmol), $B(C_6F_5)_3$ (1.50 g, 2.93 mmol) and CH_2Cl_2 (20 mL). The mixture was stirred vigorously for 20 min to form a yellow solution. The volatiles were removed under vacuum to yield a yellow solid, which was washed with benzene and dried under vacuum to yield a pale yellow solid (0.610 g, 23%). The solid (0.180 g) was suspended in toluene (8 mL) and kept still for 4 d to yield pale yellow crystalline material (0.150 g, 83%). The material that crystallized from toluene was soluble in CD_2Cl_2 for several minutes during which time ^1H and $^{31}P\{^1H\}$ NMR spectra were obtained. Subsequently, **2a** precipitated as yellow crystals. ^1H NMR (CD_2Cl_2): δ 8.08 (dd, J_{HH} = 8, J_{PH} = 5, 2H, H^3-$ArSO_3$), 7.53 (br, 8H, ArEt), 7.43 (d, J_{HH} = 8, 2H, H^4-$ArSO_3$), 7.24−7.12 (br, 6H, ArEt), 6.59 (br, 2H, ArEt), 6.72 (d, J_{PH} = 11, 2H, H^6-$ArSO_3$), 3.20−2.95 (br, overlapped, 8H, $ArCH_2CH_3$), 2.19 (br s, 6H, CH_3ArSO_3), 1.50 (br s, 6H, $ArCH_2CH_3$), 0.86 (br s, 6H, $ArCH_2CH_3$), 0.68 (s, 6H, $PdCH_3$). $^{31}P\{^1H\}$ NMR: δ 20.6 (br). Anal. Calcd. for $C_{48}H_{54}O_6P_2Pd_2S_2$(0.5 CD_2Cl_2): C, 52.51; H, 5.09. Found: C, 52.30; H, 5.19.

***Ortho*-{(3,5-^{t}Bu$_2$-Ph)$_2$P}-*para*-Toluenesulfonic Acid ((PO-3,5-^{t}Bu$_2$)H, 3b).** A flask was charged with *p*-toluenesulfonic acid (3.19 g, 18.5 mmol, dehydrated) and THF (60 mL). The mixture was cooled to 0 °C, stirred for 10 min, and BuLi (23.1 mL of a 1.6 M solution in hexanes, 37.0 mmol) was added dropwise over 3 min. The mixture was warmed to 50 °C for 10 min and then cooled to −78 °C. The dilithiated *p*-toluenesulfonic acid solution was cannula-transferred to a second flask that contained a solution of PCl_3 (1.61 mL, or 18.5 mmol) in THF (50 mL) to afford a yellow solution. A third flask was charged with Et_2O (100 mL) and 1-Br-3,5-^{t}Bu$_2$-benzene (9.97 g, 37.0 mmol), cooled to 0 °C, and BuLi (23.1 mL of a 1.6 M solution in hexanes, 37.0 mmol) was added dropwise over 3 min while the mixture was stirred. The mixture was stirred at 0 °C for 30 min, warmed to room temperature and stirred for 1 h, cooled to −78 °C, and cannula-transferred to the flask containing the Li[2-PCl_2-4-Me-benzenesulfonate]. The mixture was warmed to room temperature and stirred for 12 h to afford a bright yellow solution. The volatiles were removed under vacuum, and the residue was taken up in water (50 mL). The aqueous mixture was acidified with dilute HCl to pH∼2. The mixture was extracted with CH_2Cl_2 (3 × 50 mL), and the extracts were combined, dried over $MgSO_4$, and evaporated under vacuum to yield a yellow solid. The solid was washed with Et_2O to afford a white powder. The powder was dried under vacuum. Yield 4.51 g (42.0% based on *p*-toluenesulfonic acid). ^1H NMR ($CDCl_3$): 9.47 (d, J_{PH} = 570, 1H, P*H*), 8.30 (dd, J_{HH} = 7, J_{PH} = 5, 1H, H^3-$ArSO_3$), 7.76 (d, J_{PH} = 2, 2H, H^4-Ar-3,5-^{t}Bu$_2$), 7.57 (d, J_{PH} = 5, 1H, H^4-$ArSO_3$), 7.40 (dd, J_{HH} = 2, J_{PH} = 15, 4H, H^2-Ar-3,5-^{t}Bu$_2$), 7.04 (d, J_{PH} = 14, 1H, H^6-$ArSO_3$), 2.32 (s, 3H, *Me*$ArSO_3$), 1.28 (s, 36H, CMe_3). $^{13}C\{^1H\}$ NMR (CD_2Cl_2): δ 153.5 (d, J_{PC} = 14, C^4-Ar-3,5-^{t}Bu$_2$), 150.7 (br s, C^2-ArSO3), 140.9 (d, J_{PC} = 11, C^5-$ArSO_3$), 136.1 (s, C^4-$ArSO_3$), 134.7 (d, J_{PC} = 11, C^3-Ar-3,5-^{t}Bu$_2$), 129.6 (d, J_{PC} = 2.9, C^6-$ArSO_3$), 129.2 (d, J_{PC} = 9.4, C^3-$ArSO_3$), 128.6 (d, J_{PC} = 12, C^2-Ar-3,5-^{t}Bu$_2$), 117.7 (d, J_{PC} = 93, C^1-$ArSO_3$), 114.5 (d, J_{PC} = 92, C^1-Ar-3,5-^{t}Bu$_2$), 35.7 (s, CMe_3), 31.4 (s, CMe_3), 21.5 (s, *Me*$ArSO_3$). ^{31}P NMR (CD_2Cl_2): δ 9.8 (br s). ESI-MS (CH_2Cl_2/MeOH 1/1 by volume, negative ion scan, m/z): 580.0 ($[M - H]^-$).

dx.doi.org/10.1021/cs300147c | ACS Catal. 2012, 2, 1187−1195

{(PO-3,5-^{t}Bu$_2$)PdMe}$_2$(TMEDA) (4b). A flask was charged with (TMEDA)PdMe$_2$ (0.224 g, 0.889 mmol) and (PO-3,5-^{t}Bu$_2$)H (**3b**, 0.516 g, 0.889 mmol), and CH_2Cl_2 (30 mL) was added by vacuum transfer at −78 °C. The solution was stirred for 30 min at −78 °C, warmed slowly to room temperature, and stirred for 10 h to form a pale yellow solution. The volatiles were removed under vacuum to yield a pale yellow solid, which was washed with Et_2O (30 mL) and dried under vacuum to afford a white powder. Yield 0.560 g, 83.1%. ^{1}H NMR (CD_2Cl_2): δ 7.97 (dd, J_{HH} = 8, J_{PH} = 4, 2H, H^3-ArSO$_3$), 7.53 (s, 4H, H^4-Ar-3,5-^{t}Bu$_2$), 7.43 (dd, J_{PH} = 13, J_{HH} = 2, 8H, H^2-Ar-3,5-^{t}Bu$_2$), 7.29 (d, J_{HH} = 8, 2H, H^4-ArSO$_3$), 6.92 (d, J_{PH} = 10, 2H, H^6-ArSO$_3$), 3.63 (s, 4H, Me$_2$NC*H*$_2$C*H*$_2$NMe$_2$), 2.70 (s, 12H, *Me*$_2$NCH$_2$CH$_2$N*Me*$_2$), 2.21 (s, 6H, *Me*ArSO$_3$), 1.28 (s, 72H, C*Me*$_3$), 0.24 (d, J_{PH} = 2, 6H, Pd-*Me*). ^{13}C{^{1}H} NMR ($CDCl_3$): δ 150.9 (d, J_{PC} = 11, C^3-Ar-3,5-^{t}Bu$_2$), 146.8 (d, J_{PC} = 13, C^2-ArSO$_3$), 139.8 (d, J_{PC} = 6, C^5-ArSO$_3$), 135.2 (s, C^6-ArSO$_3$), 131.4 (s, C^4-ArSO$_3$), 129.7 (d, J_{PC} = 56, C^1-Ar-3,5-^{t}Bu$_2$), 129.7 (d, J_{PC} = 42, C^1-ArSO$_3$), 128.9 (d, J_{PC} = 13, C^2-Ar-3,5-^{t}Bu$_2$), 128.5 (d, J_{PC} = 8, C^3-ArSO$_3$), 124.7 (d, J_{PC} = 2, C^4-Ar-3,5-^{t}Bu$_2$), 59.4 (s, Me$_2$NCH$_2$CH$_2$NMe$_2$), 50.1 (s, *Me*$_2$NCH$_2$CH$_2$N*Me*$_2$), 35.3 (s, C*Me*$_3$), 31.7 (s, C*Me*$_3$), 21.5 (s, *Me*-ArSO$_3$), 1.9 (d, J_{PC} = 6, Pd-*Me*). ^{31}P{^{1}H} NMR (CD_2Cl_2): δ 30.4 (s). Anal. Calcd. for $C_{78}H_{118}N_2O_6P_2S_2Pd_2$: C, 61.69; H, 7.83; N, 1.84. Found: C, 61.96; H, 7.80; N, 1.87.

(PO-3,5-^{t}Bu$_2$)PdMe(py) (1b). A solution of (TMEDA)-PdMe$_2$ (0.885 g, 3.51 mmol) in CH_2Cl_2 (100 mL) was prepared and (PO-3,5-^{t}Bu$_2$)H (2.04 g, 3.52 mmol) was added. The mixture was stirred for 20 min at room temperature. Pyridine (1.5 mL, 17 mmol) was added, and the resulting yellow solution was stirred for 5 h to afford a pale yellow solution. The volatiles were removed under vacuum to yield a pale yellow solid, which was washed with Et_2O (30 mL) and dried under vacuum to afford a white powder. Yield 2.32 g, 84.5%. ^{1}H NMR (CD_2Cl_2): δ 8.79 (m, 2H, *o*-py), 8.05 (dd, J_{HH} = 8, J_{PH} = 4, 1H, H^3-ArSO$_3$), 7.90 (m, 1H, *p*-py), 7.55 (s, 2H, H^4-Ar-3,5-^{t}Bu$_2$), 7.52 (m, 2H, *m*-py), 7.43 (dd, J_{PH} = 13, J_{HH} = 2, 4H, H^2-Ar-3,5-^{t}Bu$_2$), 7.33 (d, J_{HH} = 8, H^4-ArSO$_3$), 6.89 (d, J_{PH} = 10, H^6-ArSO3), 2.21 (s, 3H, *Me*ArSO$_3$), 1.27 (s, 36H, C*Me*$_3$), 0.51 (d, J_{PH} = 2, 3H, Pd*Me*). ^{13}C{^{1}H} NMR (CD_2Cl_2): δ 151.4 (d, J_{PC} = 11, C^3-Ar-3,5-^{t}Bu$_2$), 150.8 (s, *o*-py), 147.5 (d, J_{PC} = 13, C^2-ArSO$_3$), 140.5 (d, J_{PC} = 6.5, C^5-ArSO$_3$), 138.9 (s, *p*-py), 135.6 (d, J_{PC} = 1.8, C^6-ArSO$_3$), 131.8 (d, J_{PC} = 2.2, C^4-ArSO$_3$), 130.0 (d, J_{PC} = 54, C^1-Ar-3,5-^{t}Bu$_2$), 129.2 (d, J_{PC} = 12, C^2-Ar-3,5-^{t}Bu$_2$), 129.1 (d, J_{PC} = 43, C^1-ArSO$_3$), 128.6 (d, J_{PC} = 8.0, C^3-ArSO$_3$), 125.7 (s, *m*-py), 125.3 (d, J_{PC} = 2.4, C^4-Ar-3,5-^{t}Bu$_2$), 35.5 (s, C*Me*$_3$), 31.6 (s, C*Me*$_3$), 21.4 (s, *Me*-ArSO$_3$), 0.7 (d, J_{PC} = 4.6, Pd*Me*). ^{31}P{^{1}H} NMR (CD_2Cl_2): δ 30.5 (s). ESI-MS (CH_2Cl_2/MeOH 1/1 by volume, positive ion scan, *m*/*z*): 417.0 (MH$^+$). Anal. Calcd. for $C_{41}H_{56}NO_3PSPd$: C, 63.11; H, 7.23; N, 1.79. Found: C, 63.04; H, 7.28; N, 1.92.

{(PO-3,5-^{t}Bu$_2$)PdMe}$_2$ (2b). A flask was charged with {(PO-3,5-^{t}Bu$_2$)PdMe}$_2$(TMEDA) (**4b**, 0.691 g, 0.455 mmol) and Et_2O (20 mL), and the mixture was vigorously stirred to form a pale yellow slurry. BF_3·(Et_2O) (0.140 mL, 1.13 mmol) was added over 2 min, and the mixture was stirred for 30 min at room temperature to afford a slightly cloudy orange solution, which was filtered through an M porosity frit. The volatiles were removed under vacuum to afford a brown solid. The solid was dissolved in benzene (5 mL) and filtered through Celite, and the filtrate was layered with hexanes (15 mL) and maintained at room temperature to afford yellow crystals after 7 days. The crystals were dissolved in CH_2Cl_2 to form a dark yellow solution. The volatiles were removed under vacuum to yield the final product as a tan powder. Yield 0.250 g, 71.3%. ^{1}H NMR (CD_2Cl_2): δ 8.11 (dd, J_{HH} = 8, J_{PH} = 4, 1H, H^3-ArSO$_3$), 7.49 (s, 2H, H^4-Ar-3,5-^{t}Bu$_2$), 7.39 (d, J_{HH} = 8, 1H, H^4-ArSO$_3$), 7.33 (d, J_{PH} = 13, 4H, H^2-Ar-3,5-^{t}Bu$_2$), 7.00 (d, J_{PH} = 10, 1H, H^6-ArSO$_3$), 2.20 (s, 3H, *Me*ArSO$_3$), 1.20 (s, 36H, C*Me*$_3$), 0.51 (s, Pd-*Me*). ^{13}C{^{1}H} NMR (CD_2Cl_2): δ 151.5 (d, J_{PC} = 14, C^3-Ar-3,5-^{t}Bu$_2$), 146.0 (s, C^2-ArSO$_3$), 141.6 (s, C^5-ArSO$_3$), 136.3 (s, C^6-ArSO$_3$), 132.5 (s, C^4-ArSO$_3$), 129.9 (d, J_{PC} = 56, C^1-Ar-3,5-^{t}Bu$_2$), 129.2 (d, J_{PC} = 14, C^2-Ar-3,5-tBu), 128.9 (d, J_{PC} = 12, C^3-ArSO$_3$), 128.4 (d, J_{PC} = 48, C^1-ArSO$_3$), 125.7 (s, C^4-Ar-3,5-^{t}Bu$_2$), 35.4 (s, C*Me*$_3$), 31.5 (s, C*Me*$_3$), 21.4 (s, *Me*-ArSO$_3$), 5.2 (s, Pd-*Me*). ^{31}P{^{1}H} NMR (CD_2Cl_2): δ 33.0 (s). APCI-MS (CH_2Cl_2, positive ion scan, *m*/*z*): 1373 (**2b** − 2Me + H$^+$)$^+$, 1387 (**2b** − Me)$^+$. Anal. Calcd. For $C_{72}H_{102}O_6P_2Pd_2S_2$: C, 61.66; H, 7.33. Found: C, 61.31; H, 7.38.

{[PO·B(C$_6$F$_5$)$_3$-3,5-^{t}Bu$_2$]PdMe}$_2$ (5b). A solution of {(PO-3,5-^{t}Bu$_2$)PdMe}$_2$ (**2b**: 0.532 g, 0.379 mmol) in CH_2Cl_2 (6 mL) was prepared, and B(C$_6$F$_5$)$_3$ (0.388 g, 0.379 mmol) was added. The mixture was stirred for 20 min at room temperature. The volatiles were removed under vacuum to yield a pale yellow solid. The solid was dissolved in hexanes and kept at −30 °C, resulting in the precipitation of a white powder, which was collected by filtration and dried under vacuum. Yield 0.581 g, 63.2%. ^{1}H NMR (CD_2Cl_2): δ 7.84 (dd, J_{HH} = 8, 1H, J_{PH} = 4, 1H, H^3-ArSO$_3$), 7.58 (s, 2H, H^4-Ar-3,5-^{t}Bu$_2$), 7.39 (d, J_{HH} = 8, 1H, H^4-ArSO$_3$), 7.22 (d, J_{PH} = 13, 4H, H^2-Ar-3,5-^{t}Bu$_2$), 6.92 (d, J_{PH} = 11, 1H, H^6-ArSO$_3$), 2.26 (s, 3H, *Me*ArSO$_3$), 1.22 (s, 36H, C*Me*$_3$), 0.72 (s, Pd-*Me*). ^{31}P{^{1}H} NMR (CD_2Cl_2): δ 34.5 (s). ^{19}F NMR (CD_2Cl_2): δ −133.8 (s, F^2), −157.6 (s, F^4), −164.5 (s, F^3). ^{11}B NMR (CD_2Cl_2): δ −1.2. Anal. Calcd. For $C_{54}H_{51}BF_{15}O_3PPdS$: C, 53.46; H, 4.24. Found: C, 53.74; H, 4.46.

[PO·B(C$_6$F$_5$)$_3$-3,5-^{t}Bu$_2$]PdMe(Et$_2$O) (6b). {[PO·B(C$_6$F$_5$)$_3$-3,5-^{t}Bu$_2$]PdMe}$_2$ (**5b**, 0.321 g, 0.264 mmol) was dissolved in Et_2O and kept at −30 °C, resulting in the precipitation of colorless crystals, which were collected by filtration and dried under vacuum. Yield 0.313 g, 92.2%. ^{1}H NMR (CD_2Cl_2): δ 7.78 (dd, J_{HH} = 8, 1H, J_{PH} = 4, 1H, H^3-ArSO$_3$), 7.55 (s, 2H, H^4-Ar-3,5-^{t}Bu$_2$), 7.35 (d, J_{HH} = 8, 1H, H^4-ArSO$_3$), 7.21 (d, J_{PH} = 13, 4H, H^2-Ar-3,5-^{t}Bu$_2$), 6.90 (d, J_{PH} = 11, 1H, H^6-ArSO$_3$), 3.67 (q, J_{HH} = 7, 4H, Et_2O), 2.25 (s, 3H, *Me*ArSO$_3$), 1.49 (t, J_{HH} = 7, 6H, Et_2O), 1.22 (s, 36H, C*Me*$_3$), 0.56 (s, Pd-*Me*). ^{31}P{^{1}H} NMR (CD_2Cl_2): δ 34.5 (s). ^{19}F NMR (CD_2Cl_2): δ −132.6 (s, F^2), −160.2 (s, F^4), −165.9 (s, F^3). ^{11}B NMR (CD_2Cl_2): δ −0.1. Anal. Calcd. For $C_{58}H_{61}BF_{15}O_4PPdS$: C, 54.11; H, 4.78. Found: C, 54.21; H, 4.84.

Reaction of {(PO-3,5-^{t}Bu$_2$)PdMe}$_2$ (2b) with Excess Ethylene. An NMR tube was charged with **2b** (14 mg, 0.010 mmol) and ferrocene (internal standard, 9 mg). CD_2Cl_2 (0.5 mL) and ethylene (86 equiv vs Pd) were added by vacuum transfer at −196 °C. The tube was warmed to −78 °C and shaken to form a pale yellow solution of (PO-3,5-^{t}Bu$_2$)PdMe-(C_2H_4) (**7b**). NMR spectra of **7b** were recorded at −40 °C. ^{1}H NMR: δ 7.95 (dd, J_{HH} = 8, J_{PH} = 4, 1H, H^3-ArSO$_3$), 7.49 (s, 2H, H^4-Ar-3,5-^{t}Bu), 7.32 (s, 1H, H^4-ArSO$_3$), 7.31 (d, J_{PH} = 13, 4H, H^2-Ar-3,5-^{t}Bu), 6.97 (d, J_{PH} = 10, H^6-ArSO$_3$), 5.42 (s, free and coordinated C_2H_4), 2.17 (s, 3H, *Me*ArSO$_3$), 1.20 (s, 36H, C*Me*$_3$), 0.34 (s, 3H, Pd*Me*). ^{13}C{^{1}H} NMR (CD_2Cl_2): δ 150.6 (d, J_{PC} = 11, C^3-Ar-3,5-^{t}Bu), 145.3 (d, J_{PC} = 13, C^2-ArSO$_3$), 140.9 (d, J_{PC} = 8, C^5-ArSO$_3$), 135.2 (s, C^6-ArSO$_3$), 131.7 (s, C^4-ArSO$_3$), 128.8 (d, J_{PC} = 56, C^1-Ar-3,5-^{t}Bu), 127.9 (d, J_{PC} = 56,

dx.doi.org/10.1021/cs300147c | ACS Catal. 2012, 2, 1187−1195

C^1-Ar-3,5-^{t}Bu), 127.7 (s, C^4-Ar-3,5-^{t}Bu), 127.5 (d, J_{PC} = 39, C^1-$ArSO_3$), 125.2 (d, J_{PC} = 2, C^3-$ArSO_3$), 120.0 (br, coordinated and free C_2H_4), 34.9 (s, CMe_3), 30.9 (s, CMe_3), 21.1 (s, *Me*-$ArSO_3$), 2.7 (s, *Me*-Pd). $^{31}P\{^1H\}$ NMR: δ 15.9 (s). The tube was warmed to 7 °C, and ethylene insertion was observed. The concentration of **7b** was determined by comparison of the integral of the Pd-*Me* resonance to that of the internal standard. After 47 min, a white precipitate had formed, and a decrease in the total integration of $[PO\text{-}3,5\text{-}^tBu_2]^-$ resonances was observed, indicating the formation of insoluble (PO-3,5-^{t}Bu$_2$)-PdR species with long alkyl chains.

Reaction of {[PO·B(C_6F_5)$_3$-3,5-^{t}Bu$_2$]PdMe}$_2$ (5b) with Excess Ethylene. An NMR tube was charged with **5b** (16 mg, 0.010 mmol). CD_2Cl_2 (0.5 mL) and ethylene (ca. 80 equiv vs Pd) were added by vacuum transfer at −196 °C. The tube was warmed to 7 °C and shaken to form a pale yellow solution of [PO·B(C_6F_5)$_3$-3,5-^{t}Bu$_2$]PdMe(C_2H_4) (**8b**). **8b** underwent rapid insertion, forming [PO·B(C_6F_5)$_3$-3,5-^{t}Bu$_2$]PdPr and [PO·B(C_6F_5)$_3$-3,5-^{t}Bu$_2$]PdEt species with concomitant formation of propene and subsequent catalytic formation of 1-butene. ^{1}H NMR of **8b**: δ 7.82 (dd, J_{HH} = 8, J_{PH} = 5, 1H, H^3-$ArSO_3$), 7.56 (s, 2H, H^4-Ar-3,5-^{t}Bu), 7.39 (d, 1H, J_{HH} = 8, H^4-$ArSO_3$), 7.15 (d, J_{PH} = 13, 4H, H^2-Ar-3,5-^{t}Bu), 6.93 (d, J_{PH} = 11, H^6-$ArSO_3$), 5.40 (s, free and coordinated C_2H_4), 2.25 (s, 3H, *Me*$ArSO_3$), 1.21 (s, 36H, CMe_3), 0.60 (d, 3H, J_{PH} = 3, Pd-*Me*). Key resonances for [PO·B(C_6F_5)$_3$-3,5-^{t}Bu$_2$]PdPr: δ 0.95 (overlapped with $CH_2{=}CH_2CH_2CH_3$, Pd−$CH_2CH_2CH_3$), 0.78 (br, Pd-$CH_2CH_2CH_3$), 0.43 (t, J_{HH} = 7, Pd-$CH_2CH_2CH_3$). Key resonances for [PO·B(C_6F_5)$_3$-3,5-^{t}Bu$_2$]Pd-Et: δ 1.51 (quintet, J_{HH} = 7, Pd-CH_2CH_3), 0.26 (q, J_{HH} = 7, Pd-$CH_2CH_2CH_3$). The concentration of **8b** was determined by comparison of the integral of the Pd*Me* resonance to that of the total integral of the *Me*$ArSO_3$ resonances (δ 2.29−2.25, no precipitate was observed). After 20 min, **5b** formed because of the depletion of ethylene.

Ethylene Oligomerization/Polymerization with [PO·B(C_6F_5)$_3$-3,5-^{t}Bu$_2$]PdMe and (PO-3,5-^{t}Bu$_2$)PdMe Catalysts (Table 1, entries 1−6). Ethylene oligomerization and polymerization reactions were performed in a 300 mL stainless steel Parr autoclave equipped with a glass linear, water cooling loop, thermocouple, and magnetically coupled stirrer and controlled by a Parr 4842 controller. In the glovebox, the catalyst was weighed into a glass autoclave linear. Toluene (50 mL) was added. The linear was placed in the autoclave, and the autoclave was assembled, brought out of the box, and hooked to the controller and to an ethylene delivery system. The reactor was heated to the desired temperature (60 °C), and stirring (200 rpm) was started. The reactor was then pressurized with ethylene. After the desired reaction time, the ethylene flow was terminated, the pressure was released, and the mixture was cooled to room temperature. The insoluble polymer products were collected by filtration, dried under vacuum, and analyzed by GPC. A small amount of the filtrate was dissolved in $CDCl_3$ and analyzed by ^{1}H NMR to determine the M_n and yield of oligomers (using ferrocene as a standard). The filtrate was also analyzed by GC-MS (Varian Saturn 2200 GC/MS/MS equipped with a VF-5 ms capillary column) to determine the molecular weight distribution of the oligomers.

Ethylene Polymerization with (PO-Et)PdMe(py)-nB(C_6F_5)$_3$ Catalysts (Table 1, entries 7−9). A stock solution of (PO-Et)PdMe(py) (**1a**, 12 mg, 0.020 mmol) and B(C_6F_5)$_3$ (1−4 equiv vs Pd) in CH_2Cl_2 (10 mL) was prepared, and 0.5 mL of the stock solution was transferred to a glass autoclave linear by syringe. The volatiles were removed under vacuum. The resulting solid was dissolved in toluene (50 mL). Polymerization was carried out using the procedure described above, except that a different temperature (80 °C) and ethylene pressure (435 psi) were used. No oligomers were detected by ^{1}H NMR analysis of the filtrates.

Polymer Characterization. Gel permeation chromatography was performed with a Polymer Laboratories PL-GPC 220 instrument using 1,2,4-trichlorobenzene solvent (stabilized with 125 ppm BHT) at 150 °C. A set of three PLgel 10 μm mixed-B LS columns was used. Samples were prepared at 160 °C. Molecular weights were determined by GPC using narrow polystyrene standards and are corrected for linear polyethylene by universal calibration using the Mark−Houwink parameters of Rudin: $K = 1.75 \times 10^{-2}$ cm^3/g and $R = 0.67$ for polystyrene and $K = 5.90 \times 10^{-2}$ cm^3/g and $R = 0.69$ for polyethylene.[48]

X-ray Crystallography. Crystallographic data are summarized in Table 2, and full details are provided in the Supporting Information. Data were collected on a Bruker Smart Apex diffractometer using Mo Kα radiation (0.71073 Å). Direct methods were used to locate many atoms from the E-map. Repeated difference Fourier maps enabled location of all expected non-hydrogen atoms. Following anisotropic refinement of all non-H atoms, ideal H atom positions were calculated. Final refinement was anisotropic for all non-H atoms and isotropic-riding for H atoms. ORTEP diagrams are drawn with 50% probability ellipsoids. Specific comments for each structure are as follows. **2a**: crystals of **2a**·2CH_2Cl_2 were obtained by crystallization from CH_2Cl_2 at room temperature. The CH_2Cl_2 molecule is partially disordered, and atoms C15, C16, C23, and C24 of the ethyl groups show positional disorder. **2b**: crystals of **2b** were obtained by crystallization

Table 2. X-ray Diffraction Data for 2a, 2b and 6b

	2a·2CH_2Cl_2	**2b**	**6b**
formula	$C_{48}H_{54}O_6P_2Pd_2S_2$ + 2CH_2Cl_2	$C_{36}H_{51}O_3PPdS$	$C_{58}H_{61}BF_{15}O_4PPdS$
formula weight	1235.62	701.20	1287.31
crystal system	monoclinic	monoclinic	monoclinic
space group	*C*2/*c*	$P2_1/c$	*C*2/*c*
a (Å)	20.009(16)	17.934(4)	36.529(7)
b (Å)	13.184(11)	10.371(2)	13.210(2)
c (Å)	19.278(16)	25.392(4)	24.939(5)
β (deg)	95.895(15)	131.536(10)	100.456(5)
V (Å^3)	5058(7)	3535.2(12)	11835(4)
Z	4	4	8
T (K)	100	100	100
crystal color, habit	pale yellow, rod	pale yellow, plate	clear, fragment
R indices ($I > 2\sigma(I)$)[a]	R1 = 0.0406	R1 = 0.0376	R1 = 0.0342
	wR2 = 0.0726	wR2 = 0.0840	wR2 = 0.0778
R indices (all data)[a]	R1 = 0.0685	R1 = 0.0505	R1 = 0.0455
	wR2 = 0.0774	wR2 = 0.0874	wR2 = 0.0808
GOF on F^2	0.893	0.942	0.955

[a] $R1 = \sum||F_o| - |F_c||/\sum|F_o|$; $wR2 = [\sum[w(F_o^2 - F_c^2)^2]/\sum[w(F_o^2)^2]]^{1/2}$, where $w = q[\sigma^2(F_o^2) + (aP)^2 + bP]^{-1}$.

from CH_2Cl_2/hexanes (1/3 v/v) at −30 °C. **6b:** crystals of **6a** were obtained by crystallization from hexanes at −30 °C. C37, C38, C39, and C40 show moderate disorder.

■ ASSOCIATED CONTENT

Supporting Information

Additional NMR data for complexes, kinetic plots, and crystallographic data for **2a**, **2b**, and **6b**. This material is available free of charge via the Internet at http://pubs.acs.org.

■ AUTHOR INFORMATION

Corresponding Author

*E-mail: rfjordan@uchicago.edu.

Author Contributions

†These authors contributed equally to this work.

Funding

This work was supported by the National Science Foundation (CHE-0911180).

Notes

The authors declare no competing financial interest.

■ ACKNOWLEDGMENTS

We thank Ian Steele for assistance with X-ray crystallography.

■ REFERENCES

(1) Nakamura, A.; Ito, S.; Nozaki, K. *Chem. Rev.* **2009**, *109*, 5215.
(2) Andreas, B.; Mecking, S. *Angew. Chem., Int. Ed.* **2008**, *47*, 2538.
(3) Drent, E.; Dijk, R.; Ginkel, R.; Oort.; Pugh, R. I. *Chem. Commun.* **2002**, 744.
(4) Drent, E.; Pello, D. H. L. European Patent 0632084, 1995.
(5) Kochi, T.; Yoshimura, K.; Nozaki, K. *Dalton Trans.* **2006**, 25.
(6) Vela, J.; Lief, G. R.; Shen, Z.; Jordan, R. F. *Organometallics* **2007**, *26*, 6624.
(7) Skupov, K. M.; Marella, P. R.; Simard, M.; Yap, G. P. A.; Allen, N.; Conner, D.; Goodall, B. L.; Claverie, J. P. *Macromol. Rapid Commun.* **2007**, *28*, 2033.
(8) Kochi, T.; Noda, S.; Yoshimura, K.; Nozaki, K. *J. Am. Chem. Soc.* **2007**, *129*, 8948.
(9) Luo, S.; Vela, J.; Lief, G. R.; Jordan, R. F. *J. Am. Chem. Soc.* **2007**, *129*, 8946.
(10) Weng, W.; Sheng, Z.; Jordan, R. F. *J. Am. Chem. Soc.* **2007**, *129*, 15450.
(11) Guironnet, D.; Roesle, P.; Runzi, T.; Gotter-Schnetmann, I.; Mecking, S. *J. Am. Chem. Soc.* **2009**, *131*, 422.
(12) Noda, S.; Nakamura, A.; Kochi, T.; Chung, L. W.; Morokuma, K.; Nozaki, K. *J. Am. Chem. Soc.* **2009**, *131*, 14088.
(13) Ito, S.; Munakata, K.; Nakamura, A.; Nozaki, K. *J. Am. Chem. Soc.* **2009**, *131*, 14606.
(14) Runzi, T.; Froehlich, D.; Mecking, S. *J. Am. Chem. Soc.* **2010**, *132*, 17690.
(15) Ito, S.; Kanazawa, M.; Munakata, K.; Kuroda, J.-I.; Okumura, Y.; Nozaki, K. *J. Am. Chem. Soc.* **2011**, *133*, 1232.
(16) Daigle, J. C.; Piche, L.; Claverie, J. P. *Macromolecules* **2011**, *44*, 1760.
(17) Nakamura, A.; Munakata, K.; Ito, S.; Kochi, T.; Chung, L. W.; Morokuma, K.; Nozaki, K. *J. Am. Chem. Soc.* **2011**, *133*, 6761.
(18) Ravasio, A.; Boggioni, L.; Tritto, I. *Macromolecules* **2011**, *44*, 4180.
(19) Tetranuclear Pd_4 catalysts based on a phosphine-bis(arenesulfonate) ligand produce polyethylene with much higher molecular weights and incorporate higher levels of vinyl fluoride in ethylene/vinyl fluoride copolymerization reactions compared to mononuclear (PO)PdMe(L) catalysts. See refs 20,21.
(20) Shen, Z.; Jordan, R. F. *J. Am. Chem. Soc.* **2010**, *132*, 52.
(21) Shen, Z.; Jordan, R. F. *Macromolecules* **2010**, *43*, 8706.
(22) (a) Komon, Z. J. A.; Bu, X.; Bazan, G. C. *J. Am. Chem. Soc.* **2000**, *122*, 1830.
(23) Komon, Z. J. A.; Bu, X.; Bazan, G. C. *J. Am. Chem. Soc.* **2000**, *122*, 12379.
(24) For recent review on activation of SHOP-type catalysts, see: Kuhn, P.; Semeril, D.; Matt, D.; Chetcuti, M. J.; Lutz, P. *Dalton Trans.* **2007**, 515.
(25) (a) Lee, B. Y.; Bazan, G. C.; Vela, J.; Komon, Z. J. A.; Bu, X. *J. Am. Chem. Soc.* **2001**, *123*, 5352.
(26) Lee, B. Y.; Bu, X.; Bazan, G. C. *Organometallics* **2001**, *20*, 5425.
(27) Boardman, B. M.; Bazan, G. C. *Acc. Chem. Res.* **2009**, *42*, 1597.
(28) Lee, B. Y.; Kim, Y. H.; Shin, H. J.; Lee, C. H. *Organometallics* **2002**, *21*, 3481.
(29) Shim, C. B.; Kim, Y. H.; Lee, B. Y.; Dong, Y.; Yun, H. *Organometallics* **2003**, *22*, 4272.
(30) Shim, C. B.; Kim, Y. H.; Lee, B. H.; Shin, D. M.; Chung, Y. K. *J. Organomet. Chem.* **2003**, *675*, 72.
(31) Kim, Y. H.; Kim, T. H.; Lee, B. Y.; Woodmansee, D.; Bu, X.; Bazan, G. C. *Organometallics* **2003**, *21*, 3082.
(32) Boardman, B. M.; Valderrama, J. M.; Munoz, F.; Wu, G.; Bazan, G. C.; Rojas, R. *Organometallics* **2008**, *27*, 1671.
(33) Brown, H. C.; Singaram, B.; Schwier, J. R. *Inorg. Chem.* **1979**, *18*, 51.
(34) Brown, H. C.; Singaram, B. *Inorg. Chem.* **1980**, *19*, 455.
(35) Shoemaker, J. A. W.; Hartman, J. S. *Can. J. Chem.* **1999**, *77*, 1856.
(36) The typical S═O and S−O bond lengths listed are for 4-Me-C_6H_4-$SO_2OCH_2CH_2$Ph: Kirby, A. J.; Parker, J. K.; Raithby, P. R. *Acta Crystallogr.* **1992**, *C48*, 832.
(37) Schaefer, W. P.; Quan, R. W.; Bercaw, J. E. *Acta Crystallogr.* **1993**, *C49*, 878.
(38) Parks, D. J.; Piers, W. E.; Parvez, M.; Atencio, R.; Zaworotko, M. J. *Organometallics* **1998**, *17*, 1369.
(39) Kreitner, C.; Geier, S. J.; Stanlake, L. J. E.; Caputo, C. B.; Stephan, D. W. *Dalton Trans.* **2011**, *40*, 6771.
(40) Flory, P. J. *J. Am. Chem. Soc.* **1940**, *62*, 1561.
(41) Schulz, G. V. *Z. Phys. Chem., Abt. B* **1935**, *30*, 379.
(42) Schulz, G. V. *Z. Phys. Chem., Abt. B* **1939**, *43*, 25.
(43) Liu, W.; Malinoski, J. M.; Brookhart, M. *Organometallics* **2002**, *21*, 2836.
(44) Malinoski, J. M.; Brookhart, M. *Organometallics* **2003**, *22*, 5324.
(45) DiRenzo, G. M.; White, P. S.; Brookhart, M. *J. Am. Chem. Soc.* **1996**, *118*, 6225.
(46) Gott, A. L.; Piers, W. E.; Dutton, J. L.; McDonald, R.; Parvez, M. *Organometallics* **2011**, *30*, 4236.
(47) Kim, Y.; Jordan, R. F. *Organometallics* **2011**, *30*, 4250.
(48) Grinshpun, V.; Rudin, A. *Makrom. Chem., Rapid Commun.* **1985**, *6*, 219.